催化学报
2012 Chinese Journal of Catalysis Vol. 33 No. 6

文章编号: 0253-9837(2012)06-0941-11 国际版 DOI: 10.1016/S1872-2067(11)60391-4 研究论文: 941~951

低温等离子体与 MnO_x/γ-Al_2O_3 协同催化降解正己醛

陈春雨, 刘 彤, 王 卉, 于琴琴, 范 杰, 肖丽萍[a], 郑小明[b]

浙江大学催化研究所, 浙江杭州 310028

摘要: 研究了在低温等离子体和催化剂共同作用下低浓度正己醛的降解反应. 结果表明, 等离子体与 γ-Al_2O_3 之间产生了很好的催化协同作用, 在低放电功率 (2.8 W) 和低温 (80 °C) 下, 干燥空气气氛中, γ-Al_2O_3 对 0.12% 正己醛的去除率为 87.1%; 当 γ-Al_2O_3 负载 7.5%MnO_x 后, 正己醛去除率达到 96.5%, 其效果与 Pt/γ-Al_2O_3 相当. 7.5%MnO_x/γ-Al_2O_3 在实验条件下连续使用 50 h, 其催化活性未见下降.

关键词: 餐饮油烟; 正己醛; γ-氧化铝; 低温等离子体; 协同作用

中图分类号: O643 **文献标识码**: A

收稿日期: 2011-12-12. **接受日期**: 2012-01-20.

[a]**通讯联系人**. **电话**: (0571)87952338; **电子信箱**: lpxiao@zju.edu.cn

[b]**通讯联系人**. **电话**: (0571)88273417; **电子信箱**: xmzheng@zju.edu.cn

基金来源: 国家自然科学基金 (J0830413); 浙江省科技厅优先主题项目 (2009C11141); 浙江省自然科学基金 (Y4090097); 浙江省创新团队项目 (2010R50014-6).

本文的英文电子版(国际版)由Elsevier出版社在ScienceDirect上出版(http://www.sciencedirect.com/science/journal/18722067).

Removal of Hexanal by Non-thermal Plasma and MnO_x/γ-Al_2O_3 Combination

CHEN Chunyu, LIU Tong, WANG Hui, YU Qinqin, FAN Jie, XIAO Liping[a], ZHENG Xiaoming[b]

Institute of Catalysis, Zhejiang University, Hangzhou 310028, Zhejiang, China

Abstract: The removal of hexanal by a combination of a non-thermal plasma and catalyst was studied. There was a synergism between the plasma and γ-Al_2O_3 that gave a hexanal removal efficiency of 87.1% at 80 °C and 2.8 W discharge power. The removal efficiency was improved to 96.5% when the γ-Al_2O_3 was loaded with 7.5% MnO_x, and a comparable efficiency was also obtained with a Pt/γ-Al_2O_3 catalyst. The 7.5%MnO_x/γ-Al_2O_3 catalyst was stable over 50 h use during which the removal efficiency did not decline.

Key words: cooking oil fume; hexanal; γ-aluminum oxide; non-thermal plasma; synergistic effect

Received 12 December 2011. Accepted 20 January 2012.

[a]Corresponding author. Tel: +86-571-87952338; E-mail: lpxiao@zju.edu.cn

[b]Corresponding author. Tel: +86-571-88273417; E-mail: xmzheng@zju.edu.cn

This work was supported by the National Natural Science Foundation of China (J0830413), the Science and Technology Department of Zhejiang Province (2009C11141), the Science Foundation of Zhejiang Province (Y4090097), and the Innovative Team Project of Zhejiang Province (2010R50014-6).

English edition available online at Elsevier ScienceDirect (http://www.sciencedirect.com/science/journal/18722067).

餐饮油烟污染逐渐引起人们的广泛关注. 餐饮油烟成份复杂, 含有多种低浓度易挥发有机物 (VOCs), 其中以正己醛最为普遍[1,2]. 它易导致肺炎, 被视为大气的三大“污染杀手”之一, 对人体和环境的危害较大[1,3,4]. 目前, 常用的油烟净化方法, 如机械分离、湿式水洗和静电分离等仅对油烟中的颗粒物具有较好的去除效果, 而对主要污染物 VOCs 去除率较低[5]. 近年来, VOCs 的脱除研究主要集中在催化燃烧法上, 即将含有 VOCs 的气体在催化剂表面进行催化燃烧, 但该法能耗高, 且常出现催化剂积炭、中毒和烧结等问题[6~10]. 因此, 如何加强新型餐饮油烟脱除技术的研究已势在必行.

低温等离子体因可在低温下活化和转化反应分子而备受关注[11~13], 但反应效率低、能耗高、目标产物选择性低. 将低温等离子体技术与催化过程相结合, 有望提高过程的能效和目标产物的选择性, 并降低反应温度. 目前低温等离子体协同催化脱除VOCs 的反应已引起越来越多的关注[14~16]. Karuppiah 等[14]在等离子体中, 以金属纤维作为高压电极, 等离子体催化降解 0.01% 的硝基苯. 他们发现, 放电区域内加入氧化钴后, 等离子体降解硝基苯能力得到较大提高, 在 22 kV 下可全部降解. Fan 等[15]和 Ding 等[16]开展了一种存储-放电循环的等离子体催化新过程脱除空气中低浓度苯和甲醛的研究, 使用的催化剂分别为 Ag/HZSM-5 和 Ag/CeO_2. 他们发现, 该方法处理极低浓度 VOCs 具有较高的催化活性、极低的能耗, 且几乎无二次污染物, 但需要储存-放电交替运行, 用于实际处理餐饮油烟极不方便.

本文将催化剂放置于介质阻挡放电等离子体的放电区间内, 即在一段式条件下 80 °C 时 (与实际烟道气温度接近) 采用等离子体与催化剂共同作用降解正己醛, 考察等离子体的放电功率、催化剂的多孔结构和比表面积、负载 MnO_x 或 Pt、MnO_x 的负载量、空速、正己醛的初始浓度和相对湿度对正己醛降解反应的影响, 并探讨了等离子体中催化剂的稳定性.

1 实验部分

1.1 催化剂的制备

实验中所用 γ-Al_2O_3 为球形商业氧化铝 (温州氧化铝厂), 它于 1100 °C 焙烧 8 h 即得 α-Al_2O_3.

采用浸渍法制备 MnO_x/γ-Al_2O_3 和 Pt/γ-Al_2O_3. 将适量四水醋酸锰 (AR, 兴塔美兴化工厂) 溶解到 1.72 ml 去离子水中, 加入 1.0 g γ-Al_2O_3, 密封、老化过夜, 在坩埚中加热炒干, 于 110 °C 干燥 2 h, 空气中 500 °C 焙烧 4 h, 即制得不同 MnO_x 负载量的 MnO_x/γ-Al_2O_3. 将 1.0 g γ-Al_2O_3 加入到 1.33 ml 20 g/L 六水氯铂酸 (AR, 国药集团化学试剂有限公司) 溶液中, 密封、老化过夜, 在坩埚中加热炒干, 于 110 °C 干燥 2 h, 空气中 500 °C 焙烧 4 h, 即制备 1% Pt/γ-Al_2O_3.

所有催化剂均经压片、筛分, 选取 20~40 目颗粒范围催化剂备用.

1.2 催化剂的表征

粉末 X 射线衍射 (XRD) 测试采用 D/MAX-RB 型 (Rigaku) XRD 仪, Cu K_α 射线源, Ni 滤光片, 管电压 40 kV、管电流 40 mA, 扫描范围 2θ = 10°~80°, 扫描速度 20°/min, 扫描步幅 0.02°.

催化剂的比表面积和孔结构在美国 Coulter Omnisorp 100CX 型物理化学吸附仪上测定. 将催化剂置于样品管中, 于 250 °C 抽真空预处理 2 h, 在液氮温度下进行的 N_2 吸附-脱附实验. 根据吸附等温线得出样品的比表面积 (BET 方程), 用 BJH 方法计算样品的孔体积和平均孔径.

采用日本 JEOL 公司的 JEM-200 型透射电子显微镜 (TEM) 观察 γ-Al_2O_3 上金属的表面分散情况. 样品经环氧树脂包埋、超薄切片后, 挂在金属铜网上观察, 并拍摄照片, 加速电压 80 kV, 放大倍数在 1.5×10^4~20×10^4.

1.3 正己醛的降解反应

反应系统如图 1 所示, 钢瓶中气体 79%N_2 +

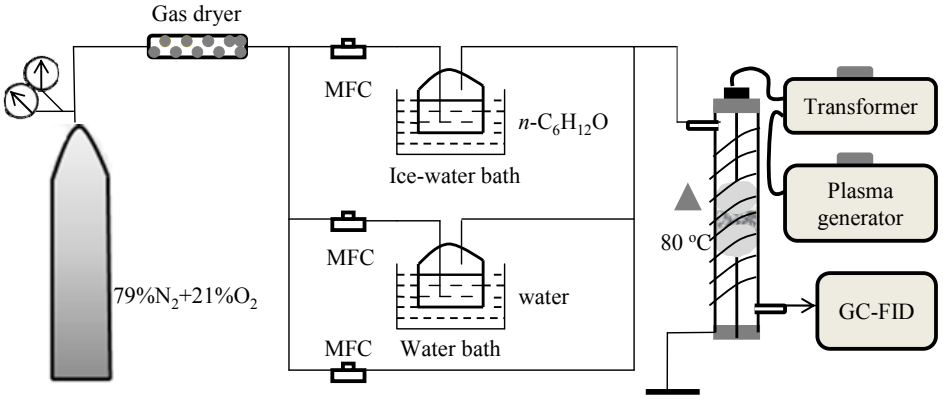

图 1 反应体系示意图

Fig. 1. Schematic diagram of the reactor system.

21%O_2 (今工气体有限公司) 经过干燥器, 用 MT50-3J 型质量流量控制器 (北京汇博隆仪器有限公司) 控制流量, 进入冰水浴的正己醛鼓泡瓶和低温恒温水浴 (杭州惠创仪器设备有限公司) 的水汽鼓泡瓶, 通过调节鼓泡气体和稀释气体的流量控制正己醛浓度和混合气的湿度. 这样模拟的含低浓度正己醛的混合气进入等离子体反应管中进行反应.

本文采用介质阻挡放电反应器, 内径 9.0 mm 的石英管为反应器并作为阻挡介质, 管心置直径为 3.0 mm 的不锈钢棒为高压电极, 石英管外包裹不锈钢丝网为接地电极. 反应管置于可开启式管式电阻炉中, 温度由 708P 型程序升温控制仪 (厦门宇光电子有限公司) 控制, 由于餐饮排气通常有一定的温度, 故本文反应温度均控制在 80 °C. 不锈钢高压电极棒与 CTP-2000K 型等离子体发生器 (南京苏曼电子有限公司) 和 TDGC2-1 型变压器 (浙江省正泰电器股份有限公司) 相连, 通过等离子发生器调节放电电流和变压器调节放电电压, 从而调节反应时等离子体的放电功率, 通过示波器法测量等离子体的实际放电功率, 等离子体的放电频率约为 9 kHz. 等离子体与催化剂协同催化反应中, 催化剂填充入等离子体放电区域中间 (一段式), 催化剂两端用石英棉固定, 催化剂填充量均为 0.1 g.

正己醛去除率由下式计算: $X = (c_0 - c)/c_0 \times 100\%$. 其中, c_0 和 c 分别为反应前后正己醛的浓度. 正己醛浓度通过气相色谱 (FuLi, GC-9790) 检测. 色谱工作条件: 色谱柱为毛细管柱, FID 检测器, 进样器温度 250 °C, 柱温 140 °C, 检测器温度 280 °C.

2 结果与讨论

2.1 无催化剂和以 γ-Al_2O_3 为催化剂时正己醛的降解反应

本文首先考察了在无催化剂填充和以 γ-Al_2O_3 为催化剂时, 等离子体中正己醛的降解反应, 结果见图 2. 可以看出, 在等离子体反应中, 当放电功率较低时, 正己醛基本不降解; 随着放电功率的增加, 正己醛去除率逐渐提高. 然而 γ-Al_2O_3 催化剂的加入使得正己醛去除率显著提高; 当放电功率为 2.8 W 时, 正己醛的去除率达到 87.1%. 而在该条件下单纯等离子体反应时只有 7.1%, 单独 γ-Al_2O_3 存在时正己醛去除率为 0. 由此可见, 在降解正己醛反应中,

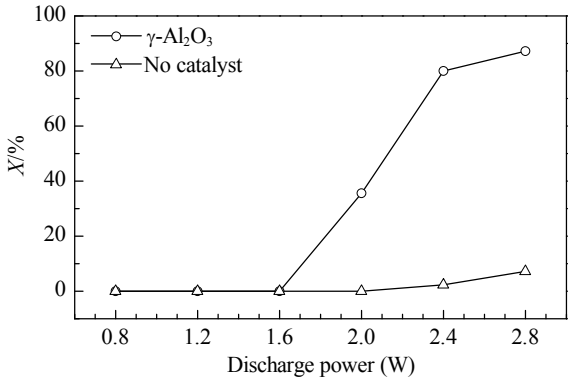

图 2 无催化剂和以 γ-Al_2O_3 为催化剂时等离子体中正己醛的去除率

Fig. 2. Removal efficiency for n-$C_6H_{12}O$ without catalyst and with γ-Al_2O_3 as catalyst. Reaction conditions: gas flow rate 100 ml/min, relative humidity 0, 0.12% n-$C_6H_{12}O$.

等离子体和 γ-Al_2O_3 间存在着显著的协同效应.

在 79%N_2 + 21%O_2 气氛下, 等离子体放电过程中会产生多种活性粒子如 O_3、活化的 N_2 分子、活化的 O_2 分子、O^+、O^-、$O(^1D)$、$O(^3P)$ 和电子等 [7,14,17]. 它们可以与进入等离子体放电区域的正己醛分子进行有效碰撞使之活化, 并发生解离和氧化, 最终完全氧化为 CO_2 和 H_2O. 由此可知, 决定正己醛降解的关键因素是正己醛分子与等离子体放电产生的活性粒子的数目和有效碰撞几率, 有效碰撞的几率越大, 正己醛的去除率越高.

当放电功率比较低时, 产生的活性粒子很少甚至没有, 极少数的活性粒子也不具有足够的能量, 使得有效碰撞的几率非常低; 随着等离子体放电功率的增加, 具有足够能量的活性粒子密度也增加, 有效碰撞的几率增大, 正己醛的去除率有所提高. 在单纯低温等离子体中, 等离子体主要由气相放电产生, 在它的作用下, 正己醛分子与活性粒子有效碰撞的几率有限, 因此正己醛的去除率较低; 在等离子体与 γ-Al_2O_3 共同作用时, 等离子体的产生由气相放电为主转变为固体表面放电为主, 放电反应过程中产生的活性粒子和正己醛分子均可以到达或吸附和富集在 γ-Al_2O_3 表面, 从而大大提高了二者的有效碰撞几率; 而随着放电功率的提高, 活性粒子密度增加, 因而正己醛的去除率明显提高.

2.2 催化剂多孔结构和比表面积对等离子体中正己醛降解反应的影响

为探讨催化剂多孔结构和比表面积对反应的影

响, 分别以 γ-Al_2O_3 和 α-Al_2O_3 为催化剂, 考察了它们在低温等离子体中正己醛降解反应中的催化效果, 结果示于图 3, 表 1 是各催化剂结构性质.

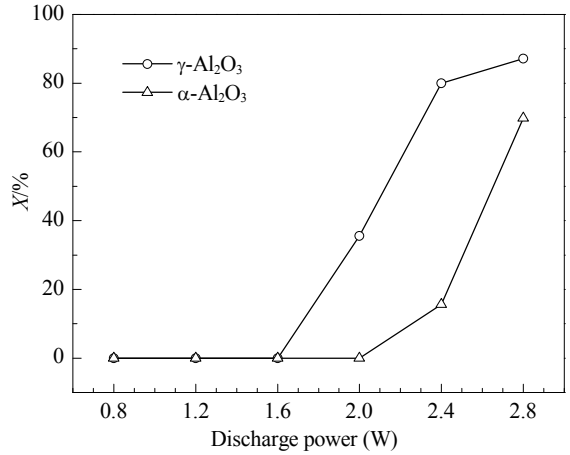

图 3 不同催化剂上正己醛的降解效果

Fig. 3. Removal efficiency of *n*-$C_6H_{12}O$ with different catalysts. Reaction conditions: gas flow rate 100 ml/min, relative humidity 0, 0.12% *n*-$C_6H_{12}O$.

表 1 各种催化剂的比表面积、孔体积和平均孔径

Table 1 Specific surface area, pore volume, and average diameter of the catalysts

Catalyst	Specific surface area (m^2/g)	Pore volume (cm^3/g)	Average diameter (nm)
α-Al_2O_3	51	0.176	16.5
γ-Al_2O_3	161	0.676	16.4
1%Pt/γ-Al_2O_3	142	0.648	16.9
5%MnO_x/γ-Al_2O_3	141	0.650	17.8
7.5%MnO_x/γ-Al_2O_3	131	0.622	18.2
10%MnO_x/γ-Al_2O_3	120	0.584	18.0
15%MnO_x/γ-Al_2O_3	115	0.533	17.5

由图可见, 随着等离子体放电功率的增加, 比表面积和孔体积较大的 γ-Al_2O_3 对正己醛的去除率明显高于比表面积和孔体积较小的 α-Al_2O_3, 如放电功率为 2.4 W 时, γ-Al_2O_3 和 α-Al_2O_3 对正己醛的去除率分别为 80.0% 和 15.6%. 这表明催化剂的多孔结构有利于等离子体中正己醛降解反应的进行, 与文献[18~21]结果一致, 其主要原因是由于比表面积和孔体积较大的催化剂增加了反应物和等离子放电产生的活性粒子在催化剂的表面吸附和富集的可能性, 提高二者有效碰撞的几率以及发生表面反应的可能性[20], 同时高的比表面积和大的孔体积也有利于反应物和产物在催化剂上快速吸附和脱附[21], 从而有利于正己醛降解反应的进行.

2.3 γ-Al_2O_3 上负载 MnO_x 或 Pt 对等离子体中正己醛降解反应的影响

由上可知, 在降解正己醛的反应中, γ-Al_2O_3 能与低温等离子体产生非常好的催化协同作用. 为了进一步提高 γ-Al_2O_3 的催化效果, 我们将传统的氧化催化组分 MnO_x 和 Pt 分别负载到 γ-Al_2O_3 上, 考察其在等离子体中降解正己醛的催化效果, 结果见图 4. 可以看出, 7.5%MnO_x 和 1%Pt 的负载使得 γ-Al_2O_3 催化效果均有所提高, 如当等离子体放电功率为 2.8 W 时, 正己醛的去除率从 87.1% 分别提高到 96.5% 和 98.7%, 可见, 7.5%MnO_x/γ-Al_2O_3 的催化效果与 1%Pt/γ-Al_2O_3 的相当. 而在无等离子体场存在、其他实验条件相同的情况下, 7.5%MnO_x/γ-Al_2O_3 和 1%Pt/γ-Al_2O_3 均不能使正己醛降解.

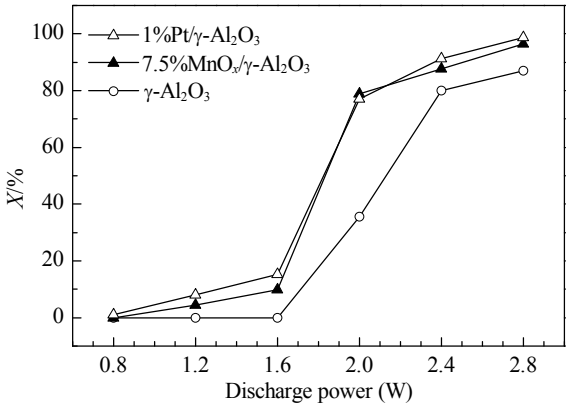

图 4 γ-Al_2O_3 上负载 MnO_x 或 Pt 对正己醛降解效果的影响

Fig. 4. Removal efficiency of *n*-$C_6H_{12}O$ with γ-Al_2O_3 after loading MnO_x or Pt. Reaction conditions: gas flow rate 100 ml/min, relative humidity 0, 0.12% *n*-$C_6H_{12}O$.

如表 1 所示, 7.5%MnO_x 和 1%Pt 负载均未使 γ-Al_2O_3 比表面积和孔体积明显降低. 从 TEM 照片(图 5(b), (f), (h) 和 (l)) 可以看出, MnO_x 和 Pt 在 γ-Al_2O_3 上分散得非常均匀, 都没有发生聚集现象. 图 6 为各催化剂的 XRD 谱. 可以看出, γ-Al_2O_3 上负载了 7.5%MnO_x 和 1%Pt 后, 均只出现 γ-Al_2O_3 的衍射峰, 而未出现 MnO_x 或 Pt 的衍射峰; 其次, 负载了 MnO_x 后, γ-Al_2O_3 的结晶度下降, 说明 MnO_x 与 γ-Al_2O_3 存在着较强的相互作用. 作者认为, 正是由于这种较强的相互作用增强了催化剂对等离子体产生的 O_3 等粒子的活化能力, 从而进一步促进了正己醛的氧化[5], 使得正己醛降解率高于 γ-Al_2O_3, 甚至与 Pt/γ-Al_2O_3 的相当.

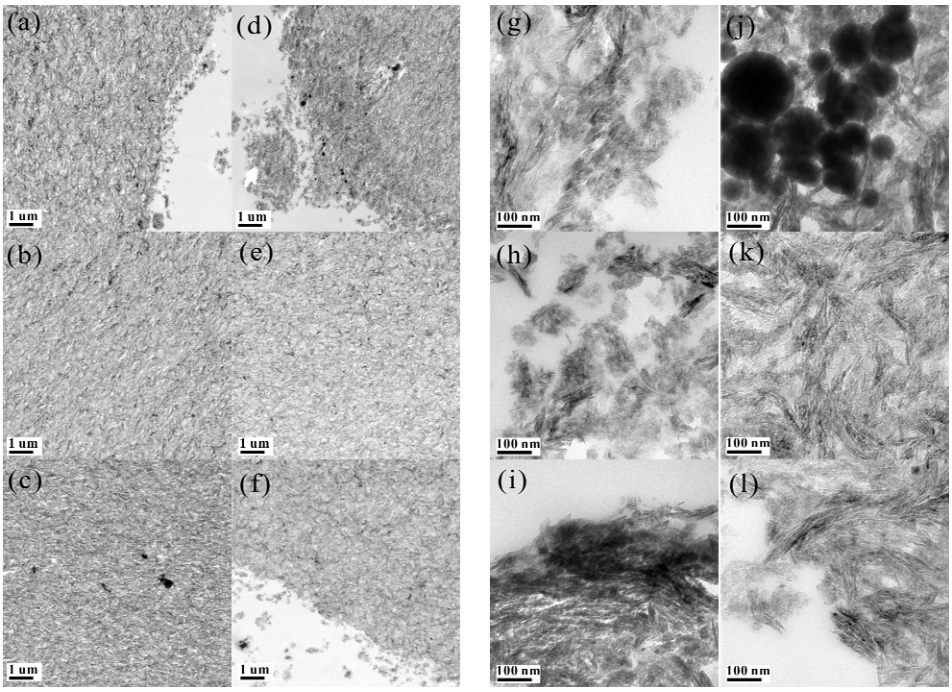

图 5 各催化剂的 TEM 照片

Fig. 5. TEM images of the various catalysts. (a, g) 5%MnO_x/γ-Al_2O_3; (b, h) 7.5%MnO_x/γ-Al_2O_3; (c, i) 10%MnO_x/γ-Al_2O_3; (d, j) 15%MnO_x/γ-Al_2O_3; (e, k) 7.5%MnO_x/γ-Al_2O_3 after reaction 50 h; (f, l) 1%Pt/γ-Al_2O_3.

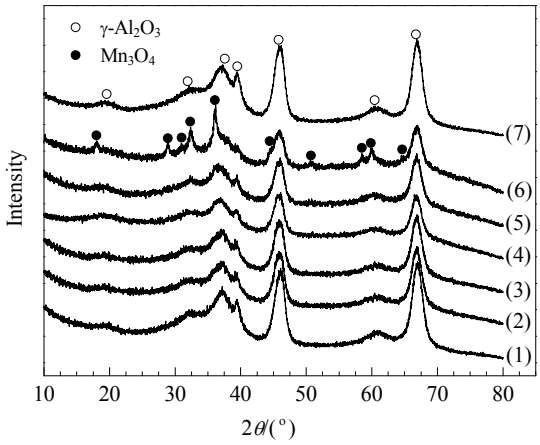

图 6 各催化剂的 XRD 谱

Fig. 6. XRD patterns of the various catalysts. (1) γ-Al_2O_3; (2) 5%MnO_x/γ-Al_2O_3; (3) 7.5%MnO_x/γ-Al_2O_3; (4) 7.5%MnO_x/γ-Al_2O_3 after reaction 50 h; (5) 10%MnO_x/γ-Al_2O_3; (6) 15%MnO_x/γ-Al_2O_3; (7) 1%Pt/γ-Al_2O_3.

2.4 γ-Al_2O_3 上 MnO_x 的负载量对等离子体中正己醛降解反应的影响

图 7 为等离子体中不同 MnO_x 负载量γ-Al_2O_3 上正己醛降解反应结果. 由图可见, 当放电功率为 2.0 W 时, 随着 MnO_x 负载量的增加, 正己醛去除率逐渐增加, 至 7.5% 时达最高, 为 78.8%. 此后继续增加 MnO_x 负载量, 正己醛去除率开始下降.

图 6 可见, 只有当 γ-Al_2O_3 上 MnO_x 负载量达到 15% 时, 才出现 Mn_3O_4 特征衍射峰, 说明 MnO_x 负载量为 10% 及以下时它在 γ-Al_2O_3 上可以分散得较均匀. 另外, 由图 5 可见, 当 MnO_x 负载量为 5% 和 7.5% 时, 它在 γ-Al_2O_3 上分散非常均匀, 未发现团聚现象; 当 MnO_x 负载量为 10% 时则出现比较明显的团聚, 至 15% 时则更为明显. 因此不难解释 7.5% MnO_x/γ-Al_2O_3 的活性最佳, 放电功率为 2.8 W 时正

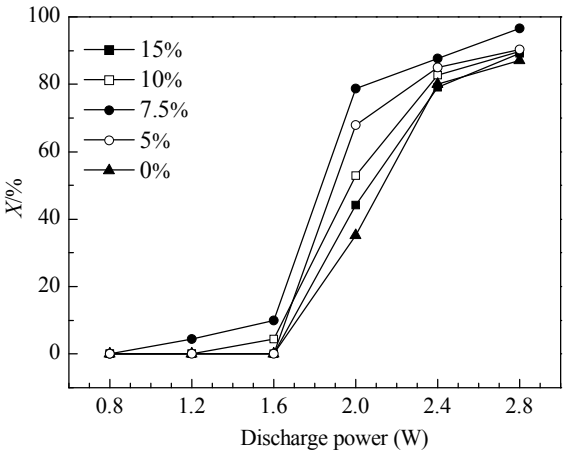

图 7 MnO_x 的负载量对正己醛去除率的影响

Fig. 7. Effect of MnO_x loading on the removal efficiency of n-$C_6H_{12}O$. Reaction conditions: gas flow rate 100 ml/min, relative humidity 0, 0.12% n-$C_6H_{12}O$.

己醛去除率可达 96.5%. 另外, 随着 MnO_x 负载量增加, 催化剂比表面积和孔体积均不断减小, 至 15% 时样品比表面积较 γ-Al_2O_3 减小了 28.6% (见表 1), 可见, 过高的 MnO_x 负载量不利于表面催化正己醛的降解反应.

2.5 空速对等离子体中正己醛降解反应的影响

由上可知, 7.5%MnO_x/γ-Al_2O_3 与等离子体协同催化效果最好, 本文在此基础上考察了空速对正己醛降解效果的影响, 结果见图 8. 可以看出, 本文所考察的空速范围内, 正己醛去除率随空速的增大而稍有减小, 总体影响不大. 由于随着空速的增大, 正己醛分子在等离子体催化区域内停留时间减少, 与放电产生的活性粒子发生有效碰撞的几率也减小, 因而正己醛去除率下降, 如当放电功率为 2.0 W 时, 在 500, 1000 和 1500 ml/(min·g) 空速下, 正己醛去除率分别为 79.7%, 78.8% 和 46.0%. 当放电功率较大时, 产生的活性粒子密度较大, 正己醛分子与活性粒子碰撞的几率受空速的影响相对较小, 因此, 正己醛去除率的变化也必然更小.

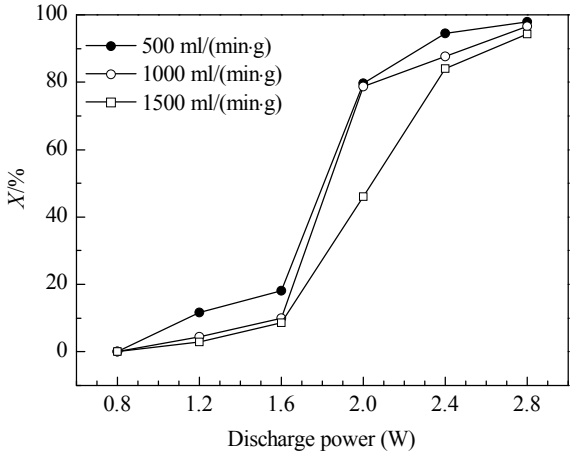

图 8 空速对正己醛去除率的影响

Fig. 8. Effect of space velocity on the removal efficiency of *n*-$C_6H_{12}O$. Reaction conditions: catalyst 7.5%MnO_x/γ-Al_2O_3, relative humidity 0, 0.12% *n*-$C_6H_{12}O$.

2.6 正己醛初始浓度对等离子体中正己醛降解反应的影响

以 7.5%MnO_x/γ-Al_2O_3 为催化剂, 考察了在相同等离子条件下正己醛初始浓度对其降解效果的影响, 结果见图 9. 可以看出, 正己醛去除率随其初始浓度的增大而减小. 由于气氛中绝大多数为载气, 等离子产生的活性粒子主要由载气生成, 其密度主要取决于放电功率. 当放电功率较小产生的活性粒子的数目有限时, 与活性粒子发生有效碰撞的正己醛分子的比例必然随着正己醛初始浓度的增加而减小, 因此正己醛去除率下降, 如当放电功率为 2.0 W 时, 正己醛初始浓度下为 0.08%, 0.12% 和 0.17% 时, 其去除率分别为 87.3%, 78.8% 和 31.5%. 当放电功率较大时, 产生的活性粒子密度较大, 正己醛分子与活性粒子碰撞的几率受正己醛初始浓度的影响相对较小, 因而正己醛去除率变化也较小, 如当放电功率为 2.8 W 时, 正己醛去除率均在 90% 以上.

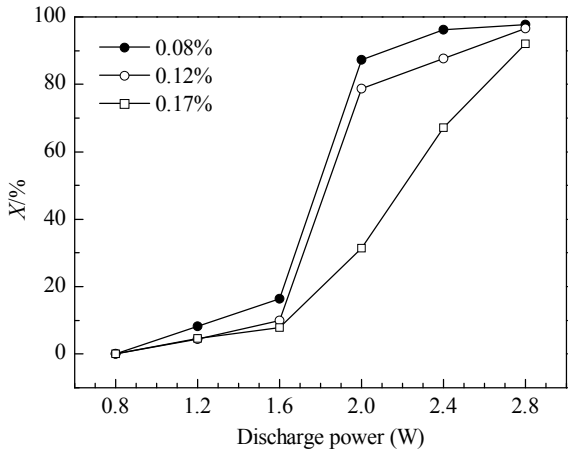

图 9 正己醛初始浓度对其去除率的影响

Fig. 9. Effect of initial concentration of *n*-$C_6H_{12}O$ on removal efficiency. Reaction conditions: catalyst 7.5%MnO_x/γ-Al_2O_3, relative humidity 0, gas flow rate 100 ml/min.

2.7 相对湿度 RH 的对等离子体中正己醛降解反应影响

水汽是餐饮油烟的重要组成部分. 因此, 本文以 7.5%MnO_x/γ-Al_2O_3 为催化剂, 考察了反应体系中 RH 对等离子体中正己醛降解反应的影响, 结果见图 10. 可以看出, 随着 RH 由 0% 逐渐增至 40%, 当放电功率为 2.0 W 时, 正己醛去除率逐渐由 78.8% 降至 13.1%, 与文献[5]所述不同. Xiang 等[5]认为, 水在介质阻挡放电过程中具有两面性: 一方面, H_2O 在等离子体场中电离产生·OH, 可促进正己醛的氧化分解; 另一方面, 水分子覆盖了催化剂表面活性位, 降低了 O_3 的产生和分解活性, 且水电离消耗电场能量, 因而正己醛去除率降低. 我们认为, RH 增加带来的不利影响大于水汽电离产生·OH 所带来的促进作用, 总体上不利于正己醛分子和活性粒子的有效碰撞, 因此正己醛的去除率仅随着 RH 的增加

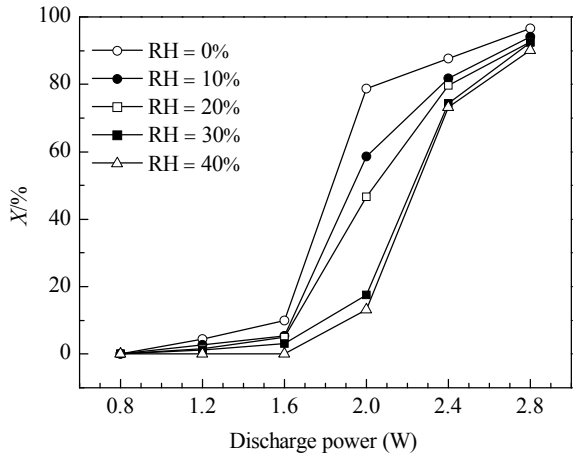

图 10 相对湿度对正己醛去除率的影响

Fig. 10. Effect of relative humidity on the conversion of *n*-$C_6H_{12}O$. Reaction conditions: catalyst 7.5%MnO_x/γ-Al_2O_3, gas flow rate 100 ml/min, 0.12% *n*-$C_6H_{12}O$.

而减小. 当放电功率较大时, 产生的活性粒子密度较大, 正己醛分子与活性粒子有效碰撞的几率受 RH 的影响较小, 正己醛的去除率变化也必然较小, 如放电功率为 2.8 W, RH 为 40% 时正己醛的去除率仍达 90.2%.

2.8 等离子体中催化剂的稳定性

综上可见, 低温等离子体降解低浓度正己醛的反应中, 7.5%MnO_x/γ-Al_2O_3 具有非常好的协同催化效果, 因此, 图 11 给出了该催化剂的稳定性. 由图可见, 在实验条件下, 7.5%MnO_x/γ-Al_2O_3 连续催化反应 50 h, 活性未见下降. 由图 6 可知, 反应前后催化剂结构基本没有变化, 仍未出现 MnO_x 衍射峰; TEM 照片 (图 5) 也显示, 反应前后催化剂上 MnO_x 的分散程度无明显差别, 其分散依然非常均匀. 由此可见, 7.5%MnO_x/γ-Al_2O_3 在等离子体催化降解正己醛反应稳定性较高. 另外, 7.5% MnO_x/γ-Al_2O_3 催化剂中未使用贵金属, 因而在降解餐饮油烟和 VOCs 中具有非常好的应用前景.

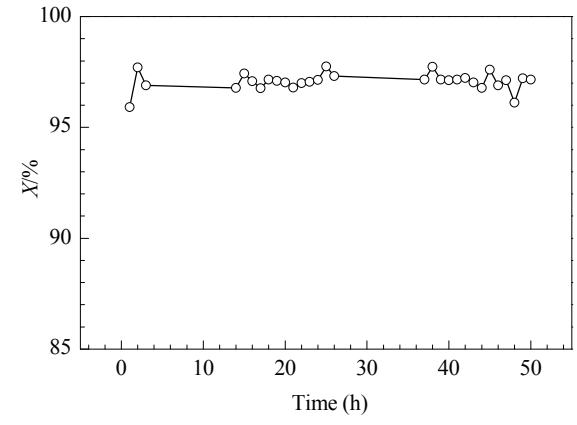

图 11 7.5%MnO_x/γ-Al_2O_3 的稳定性

Fig. 11. Stability of 7.5%MnO_x/γ-Al_2O_3. Reaction conditions: gas flow rate 100 ml/min, relative humidity 0, 0.12% *n*-$C_6H_{12}O$, discharge power 2.8 W.

3 结论

低温等离子体协同 7.5%MnO_x/γ-Al_2O_3 催化剂能有效去除餐饮油烟中主要污染物正己醛. 在低放电功率 (2.8 W) 和低温 (80 °C) 条件下, 低浓度正己醛 (0.12%) 的去除率达到 96.5%. 由于该催化剂成本低廉, 稳定性高, 因而有望应用于等离子体协同催化技术处理餐饮油烟以及 VOCs 的领域中.

参 考 文 献

1 Zhu X D, Wang K X, Zhu J L, Koga M. *J Agric Food Chem*, 2001, **49**: 4790
2 谭晓风, 孙晓钰, 刘德全, 古添发, 王仁萍. 质谱学报 (Tan X F, Sun X Y, Liu D Q, Gu T F, Wang R P. *J Chin Mass Spectrom Soc*), 2003, **24**: 270
3 Jöckel K H, Ahrens W, Wichmann H E, Becher H, Bolmaudorff U, Jahn I, Molik B, Greiser E, Timm J. *Int J Epidemiol*, 1992, **21**: 202
4 Wu S C, Yen G C. *J Food Drug Anal*, 2000, **8**: 133
5 向东, 陈颖, 赵国涛, 吴军良, 付名利, 黄碧纯, 叶代启. 环境工程学报 (Xiang D, Chen Y, Zhao G T, Wu J L, Fu M L, Huang B Ch, Ye D Q. *Chin J Environ Eng*), 2010, **4**: 1851
6 Harling A M, Glover D J, Whitehead J C, Zhang K. *Environ Sci Technol*, 2008, **42**: 4546
7 Holzer F, Roland U, Kopinke F D. *Appl Catal B*, 2002, **38**: 163
8 Spivey J J. *Ind Eng Chem Res*, 1987, **26**: 2165
9 Carpentier J, Lamonier J F, Siffert S, Zhilinskaya E A, Aboukaïs A. *Appl Catal A*, 2002, **234**: 91
10 Li W B, Wang J X, Gong H. *Catal Today*, 2009, **148**: 81
11 Schmidt J, Schnelle W, Grin Y, Kniep R. *Solid State Sci*, 2003, **5**: 535
12 Magureanu M, Mandache N B, Eloy P, Gaigneaux E M, Parvulescu V I. *Appl Catal B*, 2005, **61**: 12
13 Kim K. *Met Mater Int*, 2008, **14**: 707
14 Karuppiah J, Sivachrandiran L, Karvembu R, Subrahmanyam Ch. *Chin J Catal* (催化学报), 2011, **32**: 795
15 Fan H Y, Shi C, Li X S, Zhao D Z, Xu Y, Zhu A M. *J Phys D Appl Phys*, 2009, **42**: 22510
16 Ding H X, Zhu A M, Lu F G, Xu Y, Zhang J, Yang X F. *J Phys D: Appl Phys*, 2006, **39**: 3603
17 Van Durme J, Dewulf J, Leys C, Van Langenhove H. *Appl Catal B*, 2008, **78**: 324

18 刘彤, 于琴琴, 王卉, 蒋晓原, 郑小明. 催化学报 (Liu T, Yu Q Q, Wang H, Jiang X Y, Zheng X M. *Chin J Catal*), 2011, **32**: 1502
19 Roland U, Holzer F, Kopinke F D. *Appl Catal B*, 2005, **58**: 217
20 Wallis Anna E, Whitehead J C, Zhang K. *Appl Catal B*, 2007, **74**: 111
21 Qi G S, Yang R T. *Appl Catal B*, 2003, **44**: 217

英 译 文

English Text

Pollution by cooking oil fume is a topic of concern because it is hazardous to human health and the environment. Cooking oil fumes have complex compositions and contain low concentrations of a variety of volatile organic compounds (VOCs). Hexanal is one of the main components in cooking oil fume [1,2]. Cooking oil fumes can easily cause pneumonia, and are regarded as one of the three major "air pollution killers" [1,3,4]. Many purification methods, including mechanical separation, wet washing, and electrostatic separation, are effective for the removal of particulate matters, but they are inefficient for the removal of the major VOCs in cooking oil fumes [5]. In recent years, the removal of VOCs has focused on the catalytic combustion method, which is based on noble metal catalysts with high activity for the complete oxidation of VOCs. However, this method is limited by the cost and instability of the noble metal catalysts, which can be poisoned and sintered [6–10]. Therefore, a new technology for the removal of cooking oil fumes is needed.

The use of a non-thermal plasma (NTP) has attracted attention due to its ability to activate reactive molecules at room temperature. It can be applied in a wide range of VOCs concentration, especially concentrations lower than 0.01% [11–13]. However, its low efficiency and low CO_2 selectivity limits its industrial application. A promising approach to solve this problem is by using a combination of NTP technology with a catalyst [14–16]. Karuppiah and co-workers [14] studied the oxidative decomposition of 0.01% nitrobenzene in a catalytic plasma reactor with an inner electrode of sintered metal fibers, and found that the degradation efficiency of nitrobenzene in the plasma was much improved with a CoO_x catalyst. The selectivity for CO_2 was ~100% at 22 kV. Fan [15] and Ding [16] developed a cycled-storage-discharge (CSD) plasma catalytic process to remove dilute benzene and formaldehyde using, respectively, Ag/HZSM-5 and Ag/CeO_2 as catalyst. Their results showed that the CSD process was effective with very low concentrations of VOCs, and gave high catalytic activity and low energy consumption. However, their approach is inconvenient for the degradation of cooking oil fumes because it requires a switch storage and discharge process.

In this work, the removal of hexanal was performed using a combination of a non-thermal plasma and catalyst in one reactor (the catalyst was placed in the discharge area of the dielectric barrier discharge plasma) and at 80 °C, which is close to the gas temperature of cooking oil fumes. The factors related to efficiency, plasma discharge power, and the pore structure and surface area of the catalysts are discussed. The stability of the catalyst in the non-thermal plasma was also investigated.

1 Experimental

1.1 Catalyst preparation

Spherical commercial γ-Al_2O_3 (Wenzhou Alumina Plant) was used. α-Al_2O_3 was obtained by the further calcination of γ-Al_2O_3 at 1100 °C for 8h. MnO_x/γ-Al_2O_3 and Pt/γ-Al_2O_3 catalysts were prepared by a conventional impregnation method using γ-Al_2O_3 as catalyst support. The impregnated mixture formed by dispersing γ-Al_2O_3 powders in a $Mn(CH_3COO)_2{\cdot}4H_2O$ or $H_2PtCl_6{\cdot}6H_2O$ aqueous solution was dried at 110 °C for 2 h. The powder obtained was calcined at 500 °C for 4 h in air. All catalysts were pressed and sieved to pellets of 20–40 mesh before use.

1.2 Catalyst characterization

X-ray diffraction (XRD) patterns were recorded with a Rigaku diffractometer operated at 40 kV and 40 mA using Ni-filtered Cu K_α radiation, a step size of 0.02° and rate of 20°/min from 2θ =10° to 80°. Special surface areas were obtained from N_2 adsorption-desorption isotherms measured at –196 °C using a Coulter Omnisorp 100CX instrument. Prior to the measurement, the sample was degassed at 250 °C for 2 h in vacuum. Pore volume and average pore size were calculated from the adsorption branch of the N_2 isotherm using the Barret-Joyner-Hallenda (BJH) formula. Transmission electron microscopy (TEM) images were collected on a JEOL JEM-200 microscope operating at an acceleration voltage of 80 kV at magnification multiples of 1.5×10^4–20×10^4 to observe the dispersion of the metal or metal oxides on the surface of Al_2O_3.

1.3 Removal of Hexanal

A schematic diagram of the reactor system is shown in Figure 1. All feed gases were high purity grade (> 99.99%, Jingong Gas Co., Ltd.). The gas flow rates were controlled by MT50-3J mass flow controllers (MFC, Beijing Horiba Metron Instruments CO., LTD.). After drying by a gas dryer, the air was fed into a hexanal bubbling bottle in an ice-water bath

and a water bubbling bottle in a low temperature water bath (Hangzhou Huichuang Equipments Co., Ltd.). The concentration of hexanal and relative humidity of the mixture were controlled by the feed gas flow rate.

All experiments were carried out in a dielectric barrier discharge reactor. The reactor consisted of a dielectric barrier (a quartz tube with id 9.0 mm), a high voltage electrode (a stainless steel rod with od 3.0 mm) and a ground electrode (a stainless steel wire wrapped around the quartz tube). The reactor was placed in a tubular furnace (Shandong Longkou Xianke Instruments Co., Ltd.). The reaction temperature was kept at 80 °C by a 708P-type temperature-programmed controller (Xiamen Yuguang Electronics Co., Ltd.). The high voltage electrode rod was connected to a CTP-2000K plasma generator (Nanjing Suman Electronics Co., Ltd.) and a TDGC2-1 transformer (Zhejiang Chint Electrics Co., Ltd.). Discharge current and voltage were controlled by the plasma generator and transformer, respectively. The actual plasma discharge power was measured by the oscilloscope method. The plasma discharge frequency was 9 kHz. During the plasma-catalysis process, the catalyst was placed into the middle of the discharge area and was held by quartz cotton plugs at both ends. The amount of catalyst was 0.1 g.

The removal efficiency of hexanal was calculated by $X = (c_0 - c) / c_0 \times 100\%$, where c_0 is the initial concentration of hexanal, and c is the concentration of hexanal after reaction. The concentration of hexanal was measured by a gas chromatograph (FuLi, GC-9790) with a capillary column and FID detector using an injector temperature of 250 °C, column temperature of 140 °C and detector temperature of 280 °C.

2 Results and discussion

2.1 Effect of NTP and γ-Al_2O_3 on the removal of hexanal

The removal efficiencies of hexanal with just the plasma and just the γ-Al_2O_3 catalyst are shown in Fig. 2. Hexanal was not degraded when the discharge power was lower than 1.6 W. The removal efficiency was increased when the discharge power increased. It is noteworthy that the removal efficiency was much higher by combining the NTP with γ-Al_2O_3 than it was with either just the NTP or γ-Al_2O_3. The removal efficiency was 87.1% with the NTP and γ-Al_2O_3 at 2.8 W, which decreased to 7.1% and 0, respectively, just the NTP or just γ-Al_2O_3. This result indicated that there was a synergistic effect between the plasma and γ-Al_2O_3 in the hexanal removal reaction.

Many active species (O_3, activated N_2 molecules, activated O_2 molecules, O^+, O^-, $O(^1D)$, $O(^3P)$, and electrons) were generated in the plasma discharge in the 79% N_2 + 21% O_2 stream [7,14,17]. These active species collided with hexanal molecules in the plasma discharge area, and hexanal molecules were activated, dissociated, and oxidized. After repeated collisions, hexanal molecules were completely oxidized to CO_2 and H_2O. Therefore, the main factors in the removal of hexanal were the concentrations of hexanal molecules and active species generated by the plasma discharge, and the probability of collision between them. A higher probability of collision gives a higher removal efficiency of hexanal.

When the discharge power was low, few active species were generated, and the energy of these few active species was not high enough for effective collision. The number of active species and effective collisions increase proportionately with plasma power. In a pure NTP process, the plasma was generated by gas discharge and effective collisions between hexanal molecules and active species were limited, thus the removal efficiency of hexanal was very low. When γ-Al_2O_3 was also used with the NTP, the plasma was generated mainly by solid surface discharge, and both the active species and hexanal molecules were adsorbed on the surface of γ-Al_2O_3, which increased their effective collisions, and accounted for the excellent removal efficiency of hexanal.

2.2 Effects of pore structure and surface area of the catalyst on the hexanal removal

The effects of the pore structure and surface area of the catalyst on hexanal removal were studied by using γ-Al_2O_3 and α-Al_2O_3 as catalysts. The results are shown in Table 1 and Fig. 3. The removal efficiency with γ-Al_2O_3, which has a larger specific surface area and pore volume, was higher than that with α-Al_2O_3, which has a smaller surface area and pore volume. At 2.4 W discharge power, the removal efficiencies by γ-Al_2O_3 and α-Al_2O_3 were 80.0% and 15.6%, respectively, indicating that the porous nature of the catalyst played a positive effect [18–21]. The positive effect was due to the large surface area and pore volume increase the adsorption and concentrations of reactant molecules and active species, and subsequently increased effective collisions and surface reaction between the reactant molecules and active species [20,21].

2.3 Effect of γ-Al_2O_3 loaded with MnO_x or Pt on the hexanal removal

It was shown that there was a synergistic function between the plasma and γ-Al_2O_3 in the NTP-catalysis process. To further improve the removal efficiency, the effects of loading MnO_x and Pt on γ-Al_2O_3 were investigated. The results are shown in Fig. 4. At 2.8 W discharge power, the removal efficiencies of hexanal by MnO_x/γ-Al_2O_3 and Pt/γ-Al_2O_3

were increased from 87.1% to 96.5% and 98.7%, respectively. It was noteworthy that the catalytic activity of 7.5%MnO_x/γ-Al_2O_3 was comparable with that of 1% Pt/γ-Al_2O_3. On the other hand, in the absence of a plasma discharge, hexanal was not degraded by 7.5%MnO_x/γ-Al_2O_3 nor 1%Pt/γ-Al_2O_3 alone.

After loading 7.5% MnO_x or 1% Pt, the surface area and pore volume of γ-Al_2O_3 decreased a little (Table 1). TEM images (Figs. 5(b), (f), (h), and (l)) showed that MnO_x and Pt were dispersed on γ-Al_2O_3 uniformly and no aggregation occurred. Figure 6 is the XRD patterns of the different catalysts. After loading 7.5% MnO_x or 1% Pt on γ-Al_2O_3, only the characteristic peak of γ-Al_2O_3 appeared. The crystallinity of γ-Al_2O_3 was decreased after loading with MnO_x, implying the existence of a strong interaction between γ-Al_2O_3 and MnO_x. This strong interaction may enhance the activation of O_3 and other species and improve the removal efficiency [5].

2.4 Effect of MnO_x loading on the hexanal removal

The effect of MnO_x loading on the removal efficiency was also investigated. A series of 5%, 7.5%, 10%, and 15% MnO_x/γ-Al_2O_3 was prepared by the incipient wetness impregnation method. At 2.0 W of discharge power with 5%, 7.5%, 10%, and 15% MnO_x/γ-Al_2O_3 as catalyst, the removal efficiencies were 35.5%, 67.8%, 78.8%, 52.9%, and 44.1%, respectively. The removal efficiency of hexanal first increased with MnO_x loading. When the MnO_x loading was 7.5%, the removal efficiency reached its highest value. However, the removal efficiency decreased with further increase in the loading.

The effect of MnO_x loading was characterized by XRD (Figure 6). There was no XRD peak of MnO_x when its loading was lower than 10%, indicating that the dispersion of MnO_x on γ-Al_2O_3 was very uniform. This result was consistent with the TEM images. The characteristic XRD peaks of Mn_3O_4 appeared when the loading reached 15%. In the TEM images, obvious aggregation was found with 10% of MnO_x loading and the aggregation became more serious when the loading amount was 15%. In addition, the surface area and pore volume of 15%MnO_x/γ-Al_2O_3 were obviously decreased (from 161 to 115 g/m^2) (Table 1). These data explain the removal efficiency deterioration with an excessive MnO_x loading.

2.5 Effect of space velocity Effect of space velocity on the removal hexanal

The influence of space velocity on the removal efficiency of hexanal by 7.5% MnO_x/γ-Al_2O_3 is shown in Fig. 8. The removal efficiency declined slightly as the space velocity increased (500, 1000, and 1500 ml/(min·g)). As the space velocity increased, the residence time of hexanal molecules in the plasma catalytic area decreased, and the probability of effective collisions between hexanal molecules and active species also decreased. Therefore the removal efficiency of hexanal decreased. For example, at 2.0 W discharge power, the removal efficiency was 79.7%, 78.8%, and 46.0% for space velocities of 500, 1000, and 1500 ml/(min·g), respectively. When the discharge power was increased, the production of active species increased, and the influence of space velocity on removal efficiency was smaller.

2.6 Effect of hexanal initial concentration on the removal hexanal

The influence of hexanal initial concentration on the removal efficiency is shown in Fig. 9. The removal efficiency of hexanal decreased as the initial concentration of hexanal increased. The carrier gas accounted for most of the gas, thus active species were mainly generated from the carrier gas in the plasma, and the concentrations depended on the discharge power. At low discharge power, generated active species were limited and effective collisions between hexanal molecules and active species would decrease with increasing hexanal initial concentration, which resulted in removal efficiency deterioration. For example, at 2.0 W of discharge power, the removal efficiencies were 87.3%, 78.8%, and 31.5% for initial concentrations of 0.08%, 0.12%, and 0.17%, respectively. At 2.8 W of discharge power, the removal efficiencies were above 90% for these three initial concentrations, indicating that the influence of initial concentration became smaller when the discharge power increased.

2.7 Effect of relative humidity on the removal hexanal

Water vapor is an important component in cooking oil fume. The influence of relative humidity on removal efficiency was also investigated. The result is shown in Fig. 10. At 2.0 W of discharge power, the five relative humidities of 0%, 10%, 20%, 30%, and 40% gave removal efficiencies of 78.8%, 58.6%, 46.7%, 17.5%, and 13.1%, respectively. The removal efficiency decreased with increasing relative humidity. This was different from a previous report [5]. Xiang and co-workers [5] reported that water in the dielectric barrier discharge had two opposite effects: promoting of the oxidation of hexanal by its ionization to •OH in the plasma field and decreasing the removal efficiency by blocking catalyst active sites, reducing the generation of O_3. It is believed that the negative effect of relative humidity was larger than the positive effect in our work. In general, water vapor was detrimental to effective collisions between hexanal molecules and active species, so the removal efficiency

of hexanal decreased with increasing relative humidity. When the concentration of active species became higher with a higher discharge power, the influence of relative humidity was not significant. For example, at 2.8 W of discharge power, the removal efficiency of hexanal reached 90.2% with a relative humidity of 40%.

2.8 Stability of MnO_x/γ-Al_2O_3

The stability of MnO_x/γ-Al_2O_3 in NTP process was investigated. As shown in Fig. 11, the removal efficiency was constant when the experiment was carried out for 50 h. The XRD patterns (Fig. 6) did not show any diffraction peak of Mn_3O_4, indicating that the structure of the catalyst was not changed in the reaction. TEM images showed that the dispersion of MnO_x on γ-Al_2O_3 was still very uniform (Fig. 5) after the reaction. These results showed that the MnO_x/γ-Al_2O_3 catalyst was very stable in the NTP process. The non-thermal plasma combination with MnO_x/γ-Al_2O_3 is expected to provide new opportunities for the removal of cooking oil fume and VOCs with its high efficiency and low cost.

3 Conclusions

A non-thermal plasma in combination with a 7.5% MnO_x/γ-Al_2O_3 catalyst effectively removed hexanal. The removal efficiency of 0.12% hexanal was 96.5% at a low temperature (80 °C) and low discharge power (2.8 W). The technology with its high efficiency and low cost is expected to provide new opportunities for the removal of cooking oil fumes and VOCs.

Full-text paper available online at Elsevier ScienceDirect
http://www.sciencedirect.com/science/journal/18722067